

1-1-2000

The Effect of Various Experimental Parameters on Glow Peaks and Trapping Parameters of CaF₂:Dy (TLD-200) Crystals

A. NECMEDDİN YAZICI

M. YAKUP HACİBRAHİMOĞLU

METİN BEDİR

Follow this and additional works at: <https://journals.tubitak.gov.tr/physics>

 Part of the [Physics Commons](#)

Recommended Citation

YAZICI, A. NECMEDDİN; HACİBRAHİMOĞLU, M. YAKUP; and BEDİR, METİN (2000) "The Effect of Various Experimental Parameters on Glow Peaks and Trapping Parameters of CaF₂:Dy (TLD-200) Crystals," *Turkish Journal of Physics*: Vol. 24: No. 5, Article 5. Available at: <https://journals.tubitak.gov.tr/physics/vol24/iss5/5>

This Article is brought to you for free and open access by TÜBİTAK Academic Journals. It has been accepted for inclusion in Turkish Journal of Physics by an authorized editor of TÜBİTAK Academic Journals. For more information, please contact academic.publications@tubitak.gov.tr.

The Effect of Various Experimental Parameters on Glow Peaks and Trapping Parameters of CaF₂:Dy (TLD-200) Crystals

A. Necmeddin YAZICI, M. Yakup HACIİBRAHİMOĞLU & Metin BEDİR
*University of Gaziantep, Faculty of Engineering,
Department of Engineering Physics,
27310 Gaziantep-TURKEY*

Received 06.09.1999

Abstract

In the present study, thermoluminescence glow curves of CaF₂:Dy (TLD-200) crystals have been investigated in detail between the temperature region 300-550 K. The number of peaks and their trapping parameters (E, s and b) have been determined using the computerized glow curve fitting, peak shape and isothermal decay methods. In addition, the effect of storage times at room temperature, dose levels and heating rates on the trapping parameters have been investigated in detail by using computerized glow curve deconvolution method (CGCD) using first and general order kinetic equations.

1. Introduction

CaF₂ is one of the most carefully investigated of all thermoluminescent materials [1]. Either natural fluoride, which contains, depending on its origin, a wide variety of different impurities acting as activators, or synthetic CaF₂ as a host lattice with artificial dopants such as Tm, Dy and Mn have been used. Dysprosium-activated CaF₂ commercially available as TLD-200 from the Harshaw Chemical Co. is the most complicated in respect to glow curve structure and dose response than others [2-4].

An important consideration in the choice of a TLD is how the signal behaves in the environment in which the dosimeter is operated. Thus the thermoluminescent fading is some of the most important parameter in environmental radiation monitoring [5]. Thermal fading occurs due to the loss of charge carriers from traps. The details of the thermal fading have been understood from the values of trapping parameters. The parameters involve the number of peaks, the order of kinetics b, the activation energy E (eV) and the

frequency factor $s(s^{-1})$ of the various peaks. Additionally, these data may provide a base for a more reliable analysis of the glow curve which is necessary to derive information from the radiation quickly. Thus it is important to have a good knowledge of these parameters. There are a number of papers on the determination of the trapping parameters of LiF:Mg,Ti (TLD-100) [6-11], CaSO₄ [12-13], CaF₂:Tm and Mn [14-15], although there is no detailed information on trapping parameters of CaF₂:Dy in the literature survey [16].

In recent years, many authors (Bos *et.al.*[17], Shan-Wen Lin *et.al.*[18], Kitis *et.al.*[19], Yazici [20]) found that thermal treatments (pre-irradiation or post-irradiation), various storage times, photon energies, while cooling and heating rates have pronounced effects on the trapping parameters of most investigated TL dosimeters composed of LiF:Mg,Ti; LiF:Mg,Cu,P; CaF₂:Tm and CaF₂:MBLE. It can be concluded from the above papers that very large fluctuations can be noted for the trapping parameters calculated for the same peak for the same material. This fact would imply that comparison of trapping parameters among different experiments is not straightforward.

Therefore, the aim of the study is to determine experimentally the trapping parameters and the effects of the storage times, dose levels and also various heating rates on the glow peaks of CaF₂:Dy using a computer glow curve deconvolution program which has been the most popular method to determine the trapping parameters from the glow curves in the past years [21-27]. Additionally, the trapping parameters of the thermally isolated glow peak 6 determined by peak shape and isothermal decay. The obtained results with both methods are compared with each other. CaF₂:Dy has been chosen because of its most widely range of use in the medical and industrial areas.

2. Methods

The determination of trapping parameters from thermoluminescence glow curves has been a subject of interest for half a century. There are various methods for evaluating the trapping parameters from the glow curves [28-34]. When one glow peak is highly isolated from the others, the experimental methods such as initial rise, variable heating rates, isothermally decay, and peak shape methods are suitable methods to determine these parameters. However in most materials, the glow curve consists of several peaks, as in the CaF₂:Dy. In case of overlapping peaks there are essentially two ways to obtain these parameters, the first one is the partial thermal cleaning method and the second one is the computer glow curve deconvolution program. In most cases, the partial thermal cleaning method can not be used to completely isolate the peak of interest without any perturbation on it. Therefore, the computer glow curve deconvolution program has become very popular method to evaluate trapping parameters from TL glow curves in recent years [28-34].

2.1. Peak Shape Method

Evaluation of E from the shape of the peak utilising parameters such as T_m , full width at half-maximum $\omega = T_2 - T_1$, half width on the high temperature side of the maximum

$\delta = T_2 - T_m$, half width on the low-temperature side of the maximum $T = T_m - T_1$, and $\mu_g = \delta/\omega$ called the shape parameter.

The order of kinetics b can be estimated by means of shape parameters. Chen [29] found that μ_g is not sensitive to changes in E and s , but it changes with the order of kinetics b . It has been shown that the ranges of μ_g varies from 0.42 for $b=1$ to 0.52 for $b=2$ in case of linear heating.

The first peak shape method was developed by Grossweiner [30]; later Chen [29] modified Halperin and Braners equations [31] for calculating E values:

$$\begin{aligned} E_\tau &= [1.51 + 3(\mu_g - 0.42)] \frac{kT_m^2}{\tau} - [1.58 + 4.2(\mu_g - 0.42)] 2kT_m \\ E_\delta &= [0.976 + 7.3(\mu_g - 0.42)] \frac{kT_m^2}{\delta} \\ E_\omega &= [2.52 + 10.2(\mu_g - 0.42)] \frac{kT_m^2}{\omega} - 2kT_m \end{aligned} \quad (1)$$

After determination of the activation energy and the order of kinetics, using the following expressions the frequency factor s , it must be noted that this parameter known as a pre-exponential factor in the general order kinetic, can be estimated for first and general order kinetics respectively:

$$\begin{aligned} s &= \frac{\beta E}{kT_m^2} \exp\left[\frac{E}{kT_m}\right] \\ s &= \frac{\beta E}{kT_m^2} \left[\exp\left(-\frac{E}{kT_m}\right) (1 + (b-1) \frac{2kT_m}{E}) \right]^{\frac{b}{b-1}}. \end{aligned} \quad (2)$$

2.2. Isothermal Decay Method

The isothermal decay is quite a different method of analysis of the trapping parameters in which the TL sample temperature is kept constant and the light emission can be recorded as a function of time. Generally, in the isothermal decay method, the following equation is solved for constant T for the first order kinetics:

$$I(T) = -c \frac{dn}{dt} = c \frac{n_0}{\tau} \exp\left(-\frac{t}{\tau}\right), \quad (3)$$

where n_0 is the initial value of n and $\tau = s^{-1} \exp\left(\frac{E}{kT}\right)$.

The above equation shows that at a constant temperature T , the light emission will decay exponentially with time t and a plot of $\ln(I)$ against t will give a straight line with a slope $m = s \exp\left(-\frac{E}{kT}\right)$. In order to find E and s , the experiments are carried out at two different constant temperatures T_1 and T_2 , resulting in two different slopes m_1 and m_2 . Thus the activation energy can be determined by using the following equation:

$$E = \frac{k}{\left(\frac{1}{T_2} - \frac{1}{T_1}\right)} \ln\left(\frac{m_1}{m_2}\right). \quad (4)$$

The isothermal decay method is not applicable to higher order kinetics. In 1979, a method was proposed by Kathuria and Sunta [35] to calculate the order of kinetics from the isothermal decay of thermoluminescence. According to this method, if the decaying intensity from the sample hold at a constant temperature, the plot of $I^{(\frac{1}{b}-1)}$ versus t gives a straight line, when the proper value of b is chosen. Therefore, various b values are tried and the correct one is that giving a straight line.

2.3. CGCD Method

Computer Glow Curve Deconvolution (CGCD) is one of the most important method to determine trapping parameters from TL glow curves. This method has the advantage over experimental methods in that they can be used in largely overlapping-peak glow curves without resorting to heat treatment.

In this study, a CGCD program was used to analyse the glow curve of TLD-200. The program was developed at the Reactor Institute at Delft, The Netherlands [36]. This program is capable of simultaneously deconvoluting as many as nine glow peaks from glow curve. Two different models were used in the computer program. In the first model, the glow curve is approximated from first order TL kinetic by the expression

$$I(T) = n_0 s \exp\left(-\frac{E}{kT}\right) \exp\left[\left(-\frac{s}{\beta} \frac{kT^2}{E} \exp\left(-\frac{E}{kT}\right)\right)^*(0.9920 - 1.620 \frac{kT}{E})\right]. \quad (5)$$

In the second model the glow curve is approximated with general order TL kinetics by using the expression,

$$I(T) = n_0 s \exp\left(-\frac{E}{kT}\right) \left[1 + \left(-\frac{(b-1)s}{\beta} \frac{kT^2}{E} \exp\left(-\frac{E}{kT}\right)\right)^*(0.9920 - 1.620 \frac{kT}{E})\right]^{\frac{b}{b-1}}, \quad (6)$$

where n_0 (m^{-3}) is the concentration of trapped electrons at $t=0$, s (s^{-1}) is the frequency factor for first-order and the pre-exponential factor for the general-order, E (eV) the activation energy, T (K) the absolute temperature, k (eVK^{-1}) Boltzmann's constant, β ($^{\circ}\text{Cs}^{-1}$) heating rate and b the kinetic order.

The summation of overall peaks and background contribution can lead to composite glow curve formula as shown below:

$$I(T) = \sum_{i=1}^n I_i(T) + a + b \exp(T), \quad (7)$$

where $I(T)$ is the fitted total glow curve, a allows for the electronic noise contribution to the planchet and dosimeters infrared contribution to the background.

Starting from the above equation (7), the least square minimisation procedure and also FOM (Figure of Merit) was used to judge the fitting results as to whether they are good or not. i.e.

$$FOM = \sum_{i=1}^n \frac{|N_i(T) - I(T)|}{A} = \sum_{i=1}^n \frac{|\Delta N_i|}{A}, \quad (8)$$

where $N_i(T)$ is the i -th experimental points (total $n=200$ data points), $I(T)$ is the i -th fitted points, and A is the integrated area of the fitted glow curve.

From many experiences [37-38], it can be said that, if the values of the FOM are between 0.0% and 2.5%, the fit is good, 2.5% and 3.5% is small flow, and $> 3.5\%$ is bad fit.

To have a graphic representation of the agreement between the experimental and fitted glow curves, the computer program also plots the function,

$$X(T) = \frac{N_i(T) - I_i(T)}{\sqrt{I_i(T)}}, \quad (9)$$

which is a normal variable with an expected value 0 and $\sigma=1$ where $\sigma^2(T) = I_i(T)$.

3. Experimental Procedure

The samples used in this study were $\text{CaF}_2:\text{Dy}$ crystals TLD-200 crystal chips (3.2mm x 3.2mm x 0.38mm) obtained from Harshaw Chemical Company, Ohio, USA. The samples were annealed at 410 ± 1 °C for 30 min through the experiments to erase any residual information before the subsequent irradiation and then cooled in air at approximately 75 °C/min to room temperature. All annealing treatments were carried out with a specially designed microprocessor-controlled electrical oven. The temperature sensitivity of the oven was estimated to be ± 1.0 °C. All irradiations were performed immediately after the standard annealing at room temperature with beta rays from a $^{90}\text{Sr}-^{90}\text{Y}$ source. The irradiation equipment was an additional part of the 9010 Optical Dating System. Glow curves were obtained in a Harshaw QS 3500 manual type reader interfaced to a PC where the TL signals were analyzed. Glow curve readout was carried out on a platinum planchet at a linear heating rate of 1 °C/s, except in the case when the method of different heating rates was employed, up to 400 °C. The time duration between irradiation and TL readout was always kept constant at about 1 min, except for the storage time experiment. For each experimental study two dosimeters were used and each sample was readout twice. The second reading with the same heating profile is considered to be the background of the reader plus chip and was subtracted from the first one.

The following routine was employed in this work:

a- In the investigation of kinetic order, the samples were irradiated to various dose levels from ≈ 0.1 Gy to ≈ 110 Gy by a $^{90}\text{Sr}-^{90}\text{Y}$ beta source at a dose rate of approximately 0.02 Gy/s.

b- In order to isolate peak 6 from low temperature satellite peaks, post irradiation

annealing at 145 °C for 0, 5, 10, 14, and 20 min was performed. These annealing procedures were found after a series of experiments. The criterion was used to eliminate low temperature glow peaks with a minimum loss of intensity in the selected peak.

c- The isothermal decay measurements were performed at constant temperatures: 190 °C, 195 °C, 200 °C, 205 °C, and 210 °C after completely isolating of peak 6 from low temperature glow peaks at 145 °C for 5 min.

d- In the storage time experiments, the fading measurements were carried out with a group of 5 individually calibrated dosimeters in the following manner. After irradiation of all samples, the first of them was readout promptly, the second one was readout after 1 day and this procedure was continued with 1 day interval until reading the last sample in the group. After re-irradiation of the group, the measurements were carried out for the remaining days up to 50 days. During the experimental procedure, all samples were stored in the dark at room temperature. All the dosimeters are of the same batch and the experimental condition was kept as similar as possible.

e- In a parallel experiment to study the influence of the heating rate, linear heating rates were chosen from 1 °C/s to 20 °C/s. The heating rates below 1 °C/s was not applied, because it is not possible to obtain from our TL reader. On the other hand, at high heating rates there may be a considerable temperature lag between sample and planchet causing a difference between the measured and crystal temperature. Therefore, the upper limit of the heating rate was restricted by 20 °C/s and also thin crystals were used to minimize the temperature gradients during readout in the present study. The small temperature lags between the sample and planchet at the applied heating rates ($1^{\circ}\text{C}/\text{s} \leq \beta \leq 20^{\circ}\text{C}/\text{s}$) in the present study were also taken into consideration and the exact temperature of the sample was determined using the newly developed method by Kitis and Tuyn [39].

In all cases, the samples were irradiated to an absorbed dose of 6 Gy, except in the case when the samples were irradiated to various dose levels.

4. Results

A typical glow curve of TLD-200 sample, which is exposed to beta rays for 5 minutes after a standard annealing at 410 ± 1 °C for 30 minutes using a linear heating rate of 1 °C/s⁻¹ is shown in Figure 1. A careful investigation of this Figure allowed that, at low heating rate (<15 °C/s⁻¹), the glow curve can be described by a linear combination of six peaks between room temperature and 250 °C and also a best fit was always obtained by assuming that the first five peaks are of first-order kinetic (eq.5), and the sixth one is of general order kinetic (eq.6) [16].

The determination of both E and s mainly depends on the prior knowledge of b . Therefore, the order of kinetics of each individual glow peak was first investigated. In order to obtain the order of kinetics the following experiments was done. The reference samples were exposed to different dose levels and then glow curves measured immediately after irradiation. The results are shown in Figure 2.

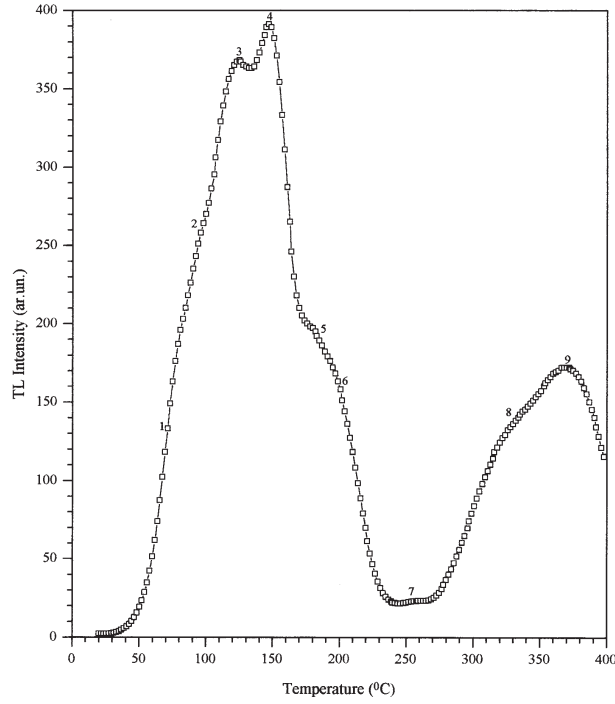


Figure 1. A typical glow curve of $\text{CaF}_2:\text{Dy}$ (TLD-200) measured after an annealing procedure of 30 min at 410°C followed by irradiation at room temperature up to 6 Gy and readout at a linear heating rate $\beta=1^\circ\text{C/s}$. In the figure open squares represent the experimental points.

In TL theory, for first order kinetics, the peak temperature of the glow peaks are expected to change only with the heating rate. Hence for a constant heating rate, the peak maxima should not be affected by other experimental parameters and should thus be fairly constant within the limit of experimental errors. However, for general order kinetics below the trap saturation points ($n_0 < N_t$), the peak temperatures are shifted to the lower temperature side with increasing the radiation exposure.

It can be seen from Figure 2 the shift in peak temperatures for the first five peaks under the different exposures is within the experimental error $\pm 2^\circ\text{C}$. This means that all of the glow peaks in the investigated region (between room temperature and 250°C) ought to be of first order kinetics. However, this is not so for peak 6 in TLD-200. Although there is no shift in the peak temperature of this peak with increasing dose levels, the CGCD program indicates that this peak can be best fitted with the general order kinetics (eq.6)[16].

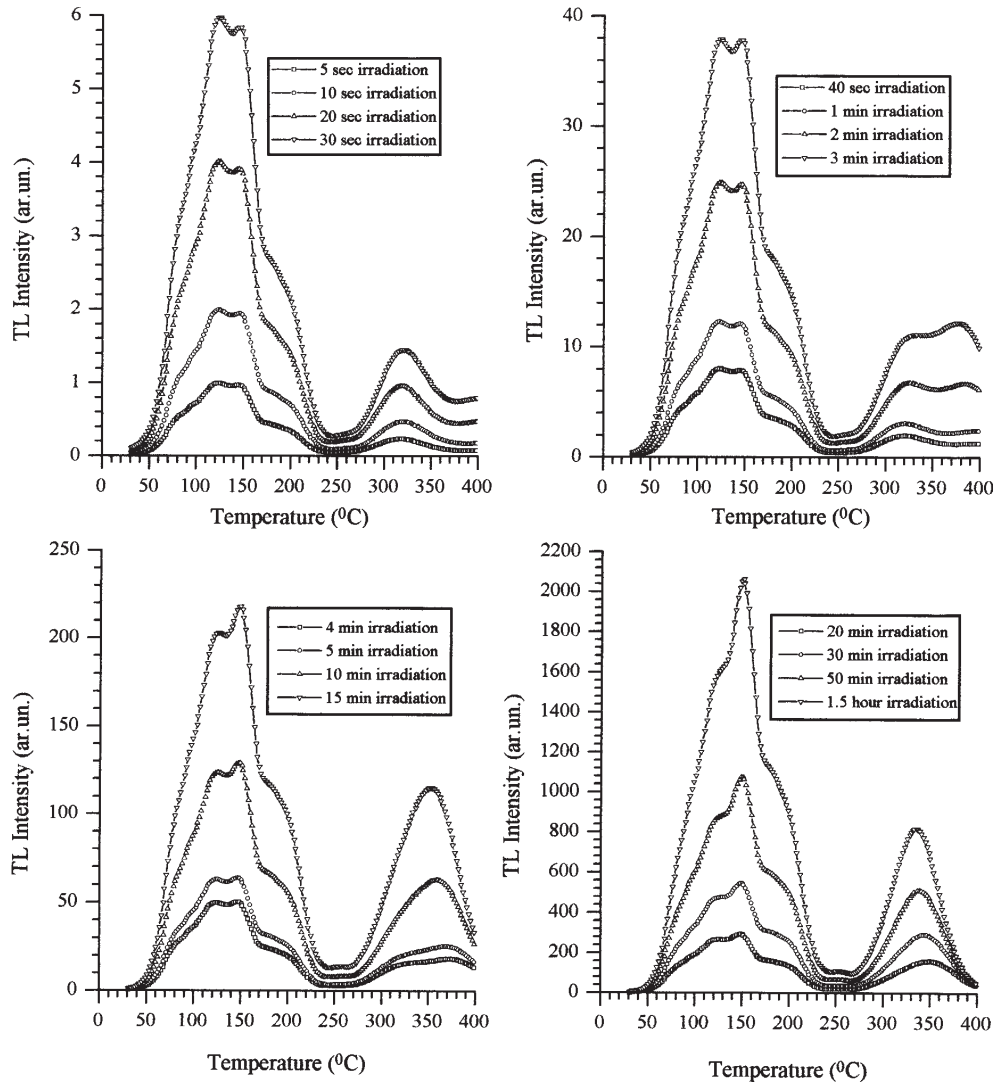


Figure 2. The glow curve of TLD-200 measured after various dose levels, at a heating rate $\beta=1$ °C/s. Doses were varied using different irradiation times at a rate of 0.02 Gy/s.

In order to understand the kinetic order of peak 6, we have also made a brief analysis of the order of kinetic of peak 6 using two methods, namely isothermal decay and the glow curve shape.

It is therefore necessary that the singleness of the peak under study must be established. In the present case, this was ascertained by recording the glow peak after partial thermal bleaching at different temperatures for different durations. The criterion used to

select the thermal treatment to erase the low temperature glow peak consisted in eliminating the influence of this low temperature glow peak with minimal loss of intensity in the selected peak. Applying this criterion, we established that after 5 min of post-irradiation thermal annealing of our sample at 145 ± 1 °C, peak 6 was isolated very well with a minimum trace of peak 5 and a minimum loss of intensity. This can be seen directly from the experimental results given in Figure 3a. Therefore, it can be conclusively said that annealing at 145 ± 1 °C for 5 min after beta irradiation removes the glow peaks I to V completely while the loss of intensity in peak 6 was limited to approximately 20%.

In order to determine the order of kinetic by means of glow curve shape method, we obtained the symmetry factor μ_g of the isolated glow peak 6. The symmetry factor μ_g of the isolated glow peaks for different annealing time at 145 ± 1 °C were calculated by taking the ratio of high temperature half-width (δ) to the total half-width (ω) and are given in Table 1 along with other parameters like the peak temperature (T_m), the low temperature half width (τ), the high temperature half-width(δ), and the full width (ω). Table 1 lists also the E and s values obtained using peak shape methods. Chen [28] found that μ_g changes with the order of kinetics b from 0.42 to 0.52, where these two limits correspond to first and second order kinetics, respectively. In the present case, μ_g has been found to be 0.462 for the isolated peak after 5 min post-annealing at 145 ± 1 °C, which gives a kinetic order of about 1.36. However, as seen from Table 1 and also from Figure 3b, when the annealing time is increased, the peak temperature has shifted to the higher temperature side and symmetry factor is increased from 0.462 to 0.495. Therefore, the present results have shown that the order of kinetics is not constant and it depends on the annealing time. This means that the order of kinetics of peak 6 increases with increasing annealing time or peak 6 is due to the continuous distribution of belonging traps.

In addition to the peak shape method, isothermal decay and CGCD method was also used to obtain the order of kinetics of peak 6. Figure 4 shows the isothermal decay at 195 °C, 200 °C, 205 °C, and 210 °C of the sample which had been annealed at 145 ± 1 °C for 5 min after beta-irradiation. Post-irradiation annealing at 145 ± 1 °C for 5 min was used to depopulate peak 5, and thereby overcome its interference with the isothermal decay of peak 6. This procedure was performed to reduce the intensity of peak 5 to less than 2% of its original intensity. An unambiguous method to ascertain that the order of kinetics followed by any given TL glow peak is first order, is to see whether the isothermal decay of the TL intensity follows an exponential law. The fact that none of these curves follows an exponential pattern is a sufficient proof against first order kinetics. Decay intensity values are normalised to 100 at $t=0$ s for all the decay. The exact value of the order of kinetics is determined by plotting the decay data in the form $I^{\frac{1}{b}-1}$ versus time for various value of b . Figure 5a shows the plots of $I^{\frac{1}{b}-1}$ versus t for various value of b . Graphs were plotted for a large number of b values at an interval of 0.05. However for clarity only three plots, for $b=1.05$, 1.2 and 1.35 are shown. The Figure 5a represents that all curves have a part of straight line. Therefore, the extraction of the order of kinetic b of peak 6 from these curves is not sufficiently possible. However, further investigations showed that b changes depending on the extent to which the trap has been populated (fig.5b). It

indicates that a straight line plot is obtained for $b=1.35$ only after about 20 s of decay has taken place. It is seen from this figure that during the initial decay of the peak, the order of kinetics is close to one. As the decay proceeds, the kinetic is found to be continuously changing and it reaches its stable value after 20 s. These values are in near agreement with the values of 1.36 determined by the peak-shape method. This means that as the decay progresses or the annealing time at $145 \pm 1 \text{ }^\circ\text{C}$ increases, more and more empty traps become available to enable an increase the retrapping.

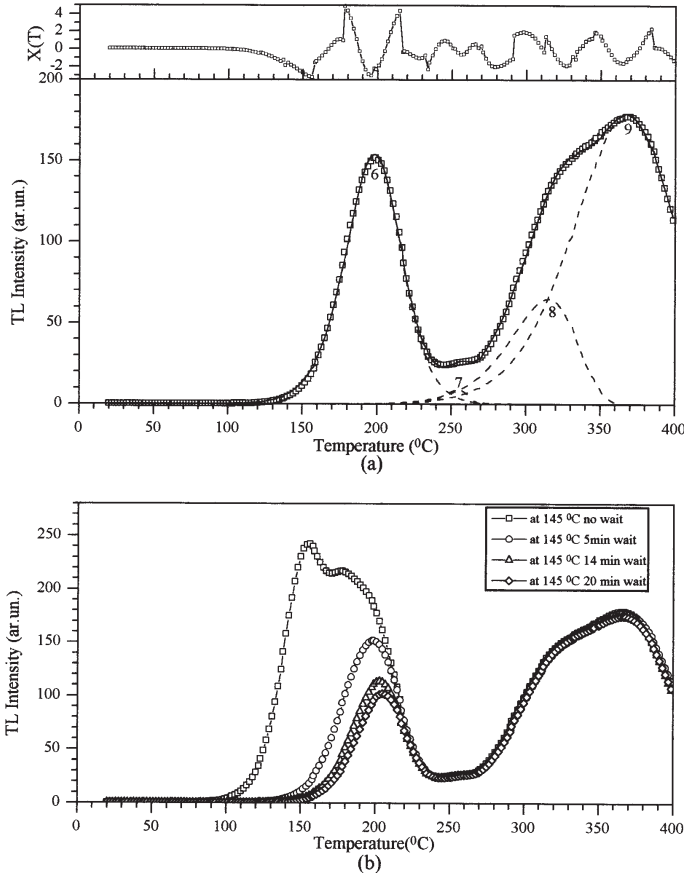


Figure 3. (a) CGCD analysed glow curve of TLD-200 following post-irradiation annealing at $145 \text{ }^\circ\text{C}$ for 5 min when neglecting peak 5 from TL glow curve. In the Figure 3-b open squares represent the experimental points, the global fitting is shown as a FOM curve and the fitted peaks are represented by broken curves. The resulting FOM was 4.7%, (b) The glow curve of TLD-200 followed post-irradiation annealing at $145 \text{ }^\circ\text{C}$ for different durations.

Table 1. Evaluated trapping parameters of glow peak 6 of TLD-200 after post-irradiation annealing procedure at 145 °C for 5, 14 and 20 min followed by readout at a linear heating rate $\beta = 1 \text{ }^\circ\text{Cs}^{-1}$. Obtained from peak-shape method.

T_1	T_m	T_2	τ	δ	ω	μ_g	b	E_τ (eV)	$E\delta$ (eV)	$E\omega$ (eV)	$\ln(s) \text{ (s}^{-1}\text{)}$
5 Min											
447.5	472	493	24.5	21	45.5	0.462	1.36	1.141	1.174	1.164	26.00
14 Min											
454.2	476	496	21.8	20	41.8	0.478	1.52	1.361	1.368	1.373	30.62
20 Min											
457.4	478	498.2	20.6	20.2	40.8	0.495	1.72	1.504	1.487	1.505	33.43

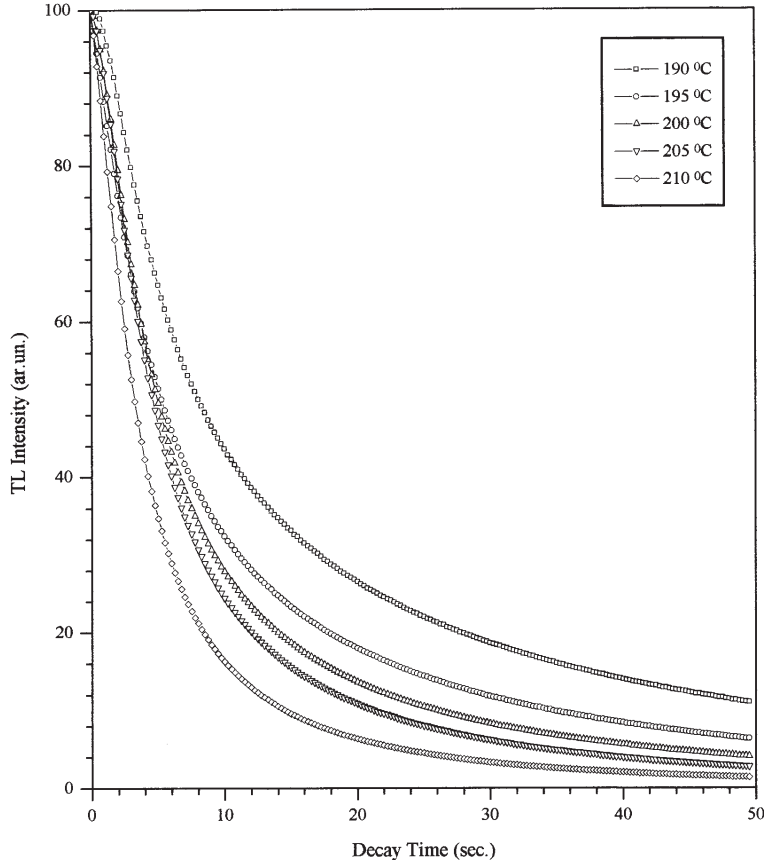


Figure 4. Normalised isothermal decay curves of isolated glow peak 6 at 190, 195, 200, 205 and 210 °C after annealing at $145 \pm 1 \text{ }^\circ\text{C}$ for 5 min. Exposure is 6 Gy in all curves.

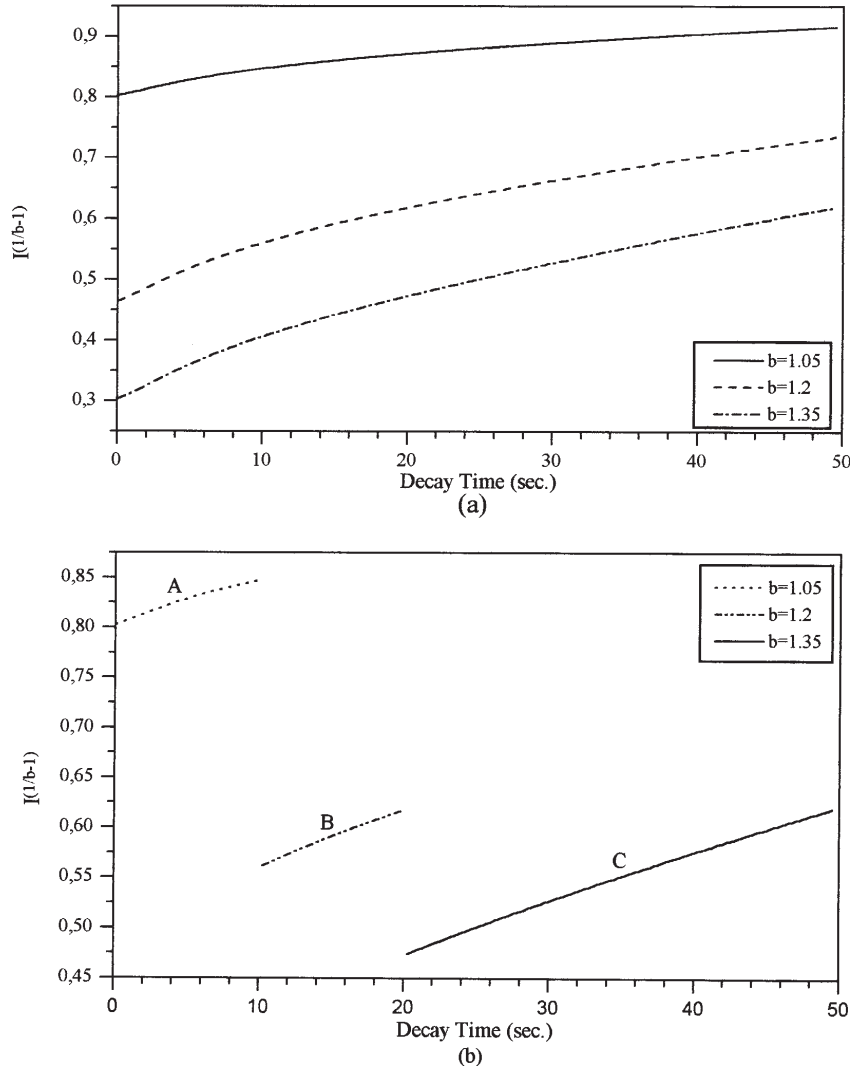


Figure 5. (a) Plots of $I^{1/(b-1)}$ versus decay time for isolated glow peak 6 for $b=1.05$, $b=1.2$ and $b=1.35$ at $195\text{ }^{\circ}\text{C}$. (b) Plots of $I^{1/(b-1)}$ versus decay time for glow peak 6 for (A) $b=1.05$, (B) $b=1.2$ and (C) $b=1.35$ for decay time 0-10 s $b=1.05$, for 10-20 s $b=1.2$, for 20-50 s $b=1.35$.

The isolated glow curves were also analysed using the CGCD program to separate peak 6 from the satellite low intensity peaks 5 and 7 in the glow curves, as well as to determine the trapping parameters of the peak including the order of kinetic of peak 6. The presence of the satellite peaks significantly complicates the investigation of trapping parameters of peak 6.

In this program, the order of kinetics is a free fitting parameter but the program includes an option to keep each parameter free or constant. The results of the computerised glow curve analysis are summarised in Table 2. The procedure has been used in this study to get a best fit. The best fit is obtained for orders of kinetic of 1.56 for the isolated glow peak after 145 ± 1 °C annealing for 5 min. The values of E and s obtained in this way were 1.26 eV and $2.05 \times 10^{12} \text{ sec}^{-1}$, respectively.

Table 2. Evaluated trapping parameters of glow peak 6 of TLD-200 after post-irradiation annealing procedure at 145 °C for 5, 14 and 20 min followed by readout at a linear heating rate $\beta = 1$ °Cs⁻¹. Obtained from computer curve fitting program.

5 Min			
E (eV)	ln(s) (s ⁻¹)	b	Peak Area (A)
1.263	28.35	1.564	1048
14 Min			
E (eV)	ln(s) (s ⁻¹)	b	Peak Area (A)
1.447	32.65	1.573	688.1
20 Min			
E (eV)	ln(s) (s ⁻¹)	b	Peak Area (A)
1.469	33.03	1.549	609.6

As seen from Figure 3, all glow peaks appear to undergo important modifications, and thereby all trap parameters following post-irradiation annealing at 145 ± 1 °C. For example, it is found that when the activation energy E changes from 1.26 to 1.47 eV, s changes from 2.05×10^{12} to $2.21 \times 10^{14} \text{ sec}^{-1}$.

So far these studies demonstrate that all of the trapping parameters, especially the kinetic order of peak 6, can change with the heat treatments after the irradiation.

4.1. Storage time experiment

An alternative experiment to extract the change in the trapping parameters can be done by storing the samples at room temperature for different period of time. In the storage time experiments, the measured glow curves are shown in Figure 6. All of them are analysed by using CGCD program. Figure 7 represents the analysed glow curves corresponding to storage times of 5 days and 45 days at room temperature and shows that there are important changes in the glow curves with respect to the normal TL glow curve in Figure 1.

Peak 1 was neglected after a 1 day storage time due to its fast fading. The trapping parameter E versus storage time for the peaks 1 to 6 are shown in Figure 8. The values of E for the analysed glow peaks are remarkably interesting. The dramatic changes start immediately and continue throughout the storage period. Peak 1 and 2 exhibit similar behaviour, their activation energies sharply increases with increasing storage time until

they disappear. Activation energy of peak 3 always increases, but the increase in the first part of storage time up to 5 days is much more significant than the later time. Peak 4 first considerably drops in the initial part of storage time and then seems to level off with some small up or down changes. On the other hand, opposite to the behaviour of peak 4, peak 5 first makes a quick rise and then slowly decreases with some fluctuations as the storage time increases. The activation energy of peak 6 is especially interesting. First it sharply decreases from 1.04 eV to 0.93 eV, it then sharply increases to 1.0 eV and then starts slowly increasing again with storage time to a value of 1.03 eV.

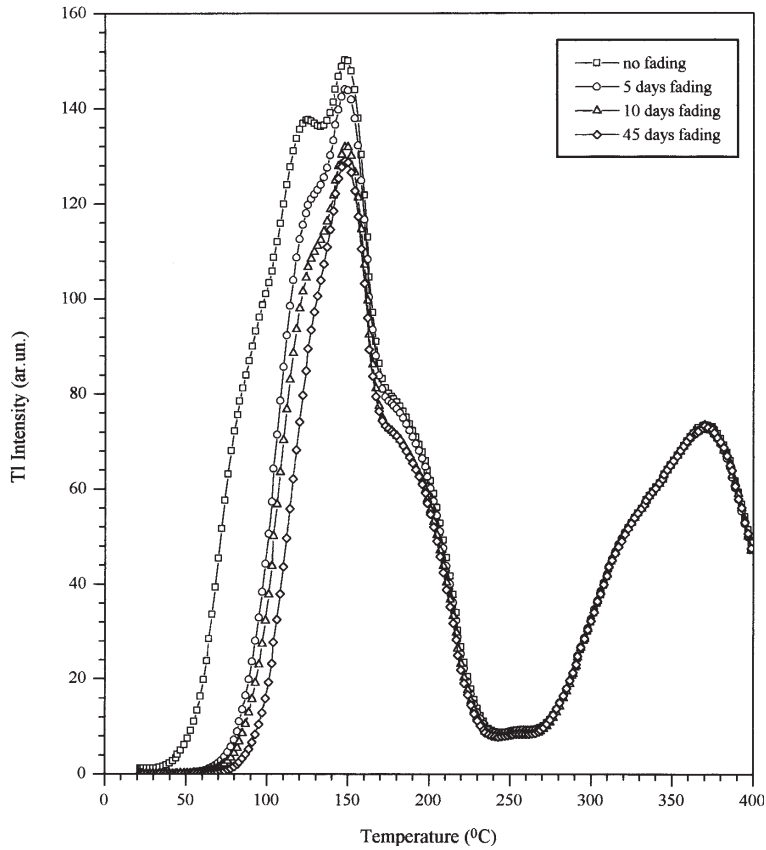


Figure 6. A set of TL glow curves for TLD-200 crystal measured after different storage times at room temperature in the dark. All glow curves were read out at 1 °C/s after the samples were exposed to an irradiation of 6 Gy.

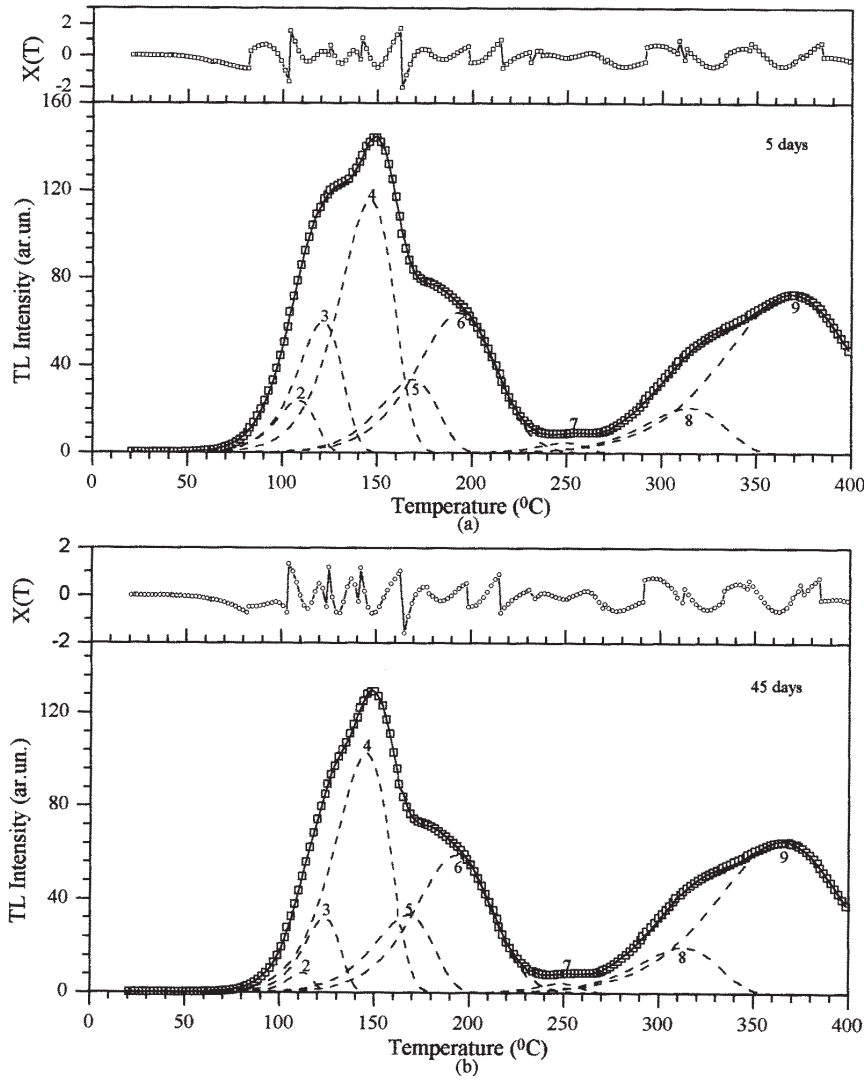


Figure 7. The CGCD analysed glow curves of TLD-200 crystal after storage at room temperature (a) for 5 days (FOM=0.72%), (b) for 45 days (FOM=0.63%). The open squares represent the experimental points, the full curve is the global fitting and broken curves represent fitted individual peaks.

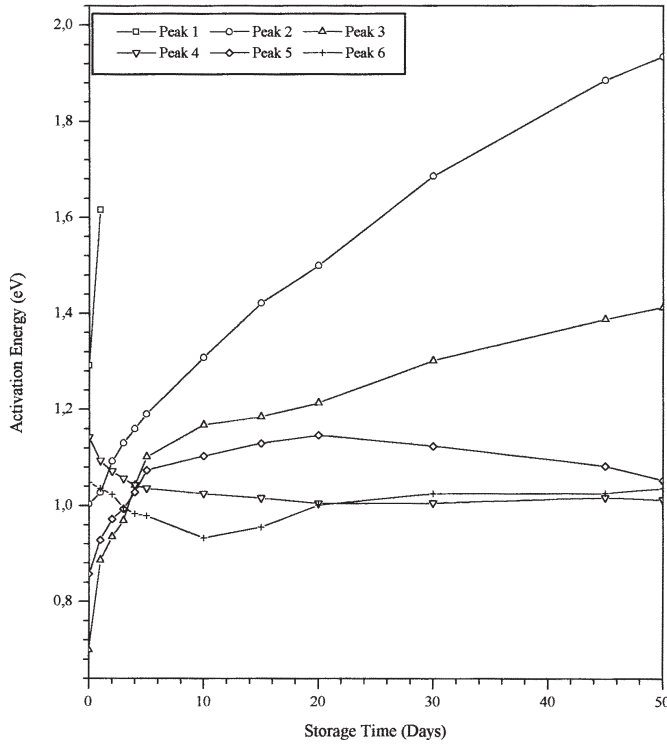


Figure 8. Activation energy determined by computerised glow curve fitting program versus storage times in the storage time experiment for glow peaks from glow curves registered at a linear heating rate 1 °C/s.

4.2. Heating Rate Experiment

The other purpose of this study is to determine whether there is any effects of heating rate on the trapping parameters by glow curve analysis. Bos *et.all.* [16] have demonstrated that heating rates have a pronounced effects on the trapping parameters of TLD-100. Therefore, heating rate is one of the most important experimental parameters which strongly effects the intensities of the TL glow curves. However, its effect frequently neglected in the experimental studies.

TL measurements allowed that glow curves measured at different heating rates have different peak maximum temperatures and different shapes. A set of measured glow curves for TLD-200 at different heating rates is shown in Figure 9. It can be seen from this figure that the peak maximum temperatures increase with heating rate but in addition, the peak positions change with respect to one another. It is instructive to see that the positions of peaks 3 and 4 are converging at the higher heating rates.

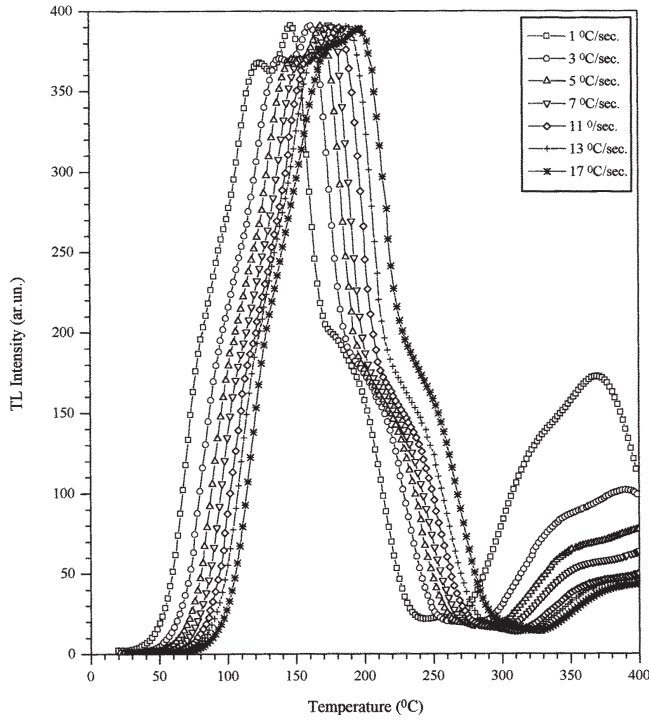


Figure 9. Some examples of arbitrary normalised glow curves of TLD-200 measured at various heating rates from 1 °C/s to 20 °C/s. In each curve the dots represent the experimental points.

Figure 10 shows some of the computer analysed glow curves which were read out at various heating rates such as 1 °C/s and 17 °C/s. The individual glow peaks resulting from the CGCD procedure are also shown in this figure. In this study, we note an interesting result on the behaviour of peak 5. As the heating rates increases, the intensity of this peak continuously decreases and for higher heating rates ($\beta > 15$ °C/s), the intensity of this peak is meanly negligible and for $\beta > 20$ °C/s, it has been completely disappeared.

The activation energies found by fitting of the glow curves recorded at various heating rates, are shown in Figure 11. As in the storage time experiment, the dramatic changes in the activation energy for all peaks start immediately and continue with increasing heating rate. Again, the activation energies of peaks 1 and 2 show similar behaviour. After some small up or down changes, their activation energies start to slowly increase from approximately, 5 °C/s and then they reach their plateau values after 15 °C/s. The E value of peak 3, as in the storage time experiment, increases continuously but the increase in the heating rates below 5 °C/s is much more significant than at heating rates above 5 °C/s. On the other hand, the activation energy of peak 4 shows an opposite behaviour due to the activation energy of peaks 3 and 5. Up to a heating rate of 8 °C/s there is

a negligible change in the activation energy of peak 4. However, after at 8 °C/s, the change in the activation energy of peak 4 starts to decrease gradually and it continues up to highest heating rate (20 °C/s). The E of peak 5 is more or less constant below the read out at 7 °C/s, but above this heating rate, there is a sudden strong increase of E with increasing heating rate until it completely disappears. Because of large increase in E of peak 5, it is represented on the secondary y-axis to observe clearly the variations in the trapping parameters of all other peaks. After a small up or down changes, E of peak 6 decreases with increasing heating rate, reaches a minimum at about 13 °C/s and increases slowly for higher values of heating rates. All in all, it can be assumed that up to approximately 6 °C/s, the E values of all peaks, except for peak 3, are constant and above this heating rate, there are pronounced variations in the trapping parameters for all glow peaks.

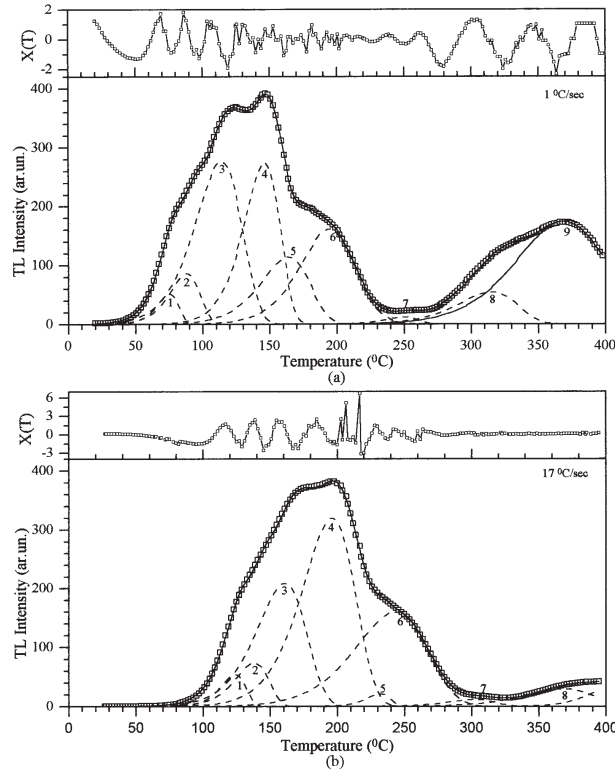


Figure 10. (a) Deconvoluted glow curve of CaF₂:Dy (TLD-200) obtained at a heating rate of 1 °C/s following β -irradiation to a dose level of 6 Gy. (b) Deconvoluted glow curve of TLD-200 under identical experimental conditions, except the heating rate which was 17 °C/s. Experimental data are indicated with open squares and individual glow peaks are indicated with dash lines. ((a) FOM=0.78%, (b) FOM=0.85%)

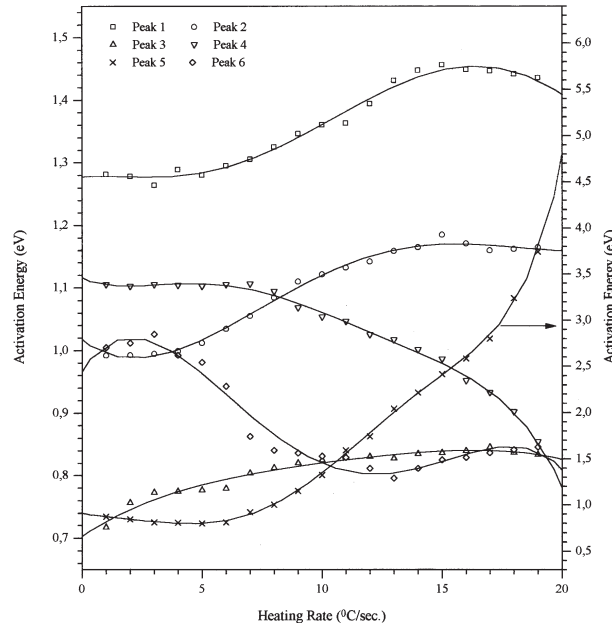


Figure 11. The activation energy determined by CGCD program against heating rate from 1 °C/s to 20 °C/s. The points shown are the average values of the E of two different samples. Lines are the fits to guide the eye.

The change in the kinetic order of peak 6 found by glow curve fitting in the heating rate experiment is shown in Figure 12. In TL theory, the kinetic order b is not depend on the heating rate. However, in this study, it was shown that the kinetic order of peak 6 has a drift phenomenon with changing heating rate. It is observed that at the beginning of the curve b is ≈ 1.35 for $\beta = 1$ °C/s. Between 1 °C/s and 7 °C/s, the value of b sharply decreases to 1.07 and then it reaches to its more or less constant value around 1.04 ± 0.02 .

The variable heating rate method was also used in the present study to determine the activation energy of some peaks in TLD-200. According to this method, for $b=1$, a plot of $\ln(T_m^2/\beta)$ versus $1/T_m$ yields a straight line of slope E/k . Once E is known the frequency factor may be obtained from the intercept of the graph on the $\ln(T_m^2/\beta)$ axis. However, it should be noted that accurate results are difficult to achieve with this method since large changes in heating rate produce relatively small shifts in the peak positions. Additionally, extra difficulty arises in the case of overlapping glow peaks, as in the TLD-200. Because, in complex type glow curves the peak temperatures T_m of some glow peaks can not be exactly distinguish from the glow curves. In some case [17], this difficulty has solved using the computerised glow curve fitting technique. However, if the turning point of glow peak (I_m) is not clear, this technique can not be sufficiently reliable to determine the peak temperatures. For the glow curves of TLD-200, the peak temperatures of peak

3 and 4 clearly distinguish from the other peaks and when we compare these values with the obtained values by CGCD, it was seen that they have approximately same values. Therefore, in the given study, we only determined the trapping parameters of glow peaks 3 and 4.

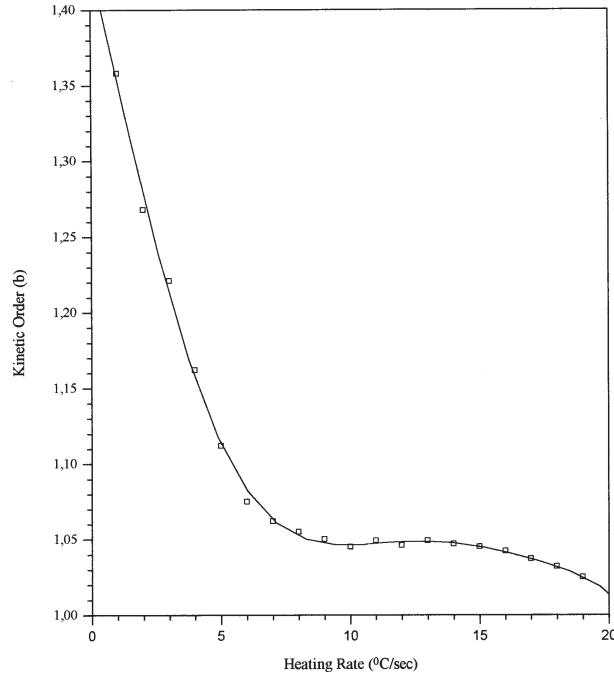


Figure 12. Variation of the kinetic order of peak 6 obtained by computerized fits as a function of heating rate from 1 °C/s to 20 °C/s.

From the T_m values obtained by CGCD, Figure 13 has been deduced. In this figure, the full lines are least squares regression fits and it is seen that large deviations from the straight line occur, especially at high heating rates (low $1/T_m$). The most important cause of these deviations is the temperature lag between the sample and planchet. In Figure 13, it is seen that the good fitted lines are through the data points for $\approx \beta < 6$ °C/s. The E values determined from the slopes of those lines are 0.88 eV and 1.12 eV for the peaks 3 and 4, respectively. So we can conclude that for glow peak 4, the determined E value by variable heating rate method and found by glow curve fitting method between $\beta=1$ °C/s and 6 °C/s are more or less consistent with each other. However, this does not hold for glow peak 3 whose E value according to variable heating rate method is higher than all values determined by glow curve fitting method but the differences are small at high heating rates than lower heating rates. These differences are probably rise from its overlapping neighbour peaks, band-width variations with increasing heating rates and also its intensity decrease with increasing heating rates.

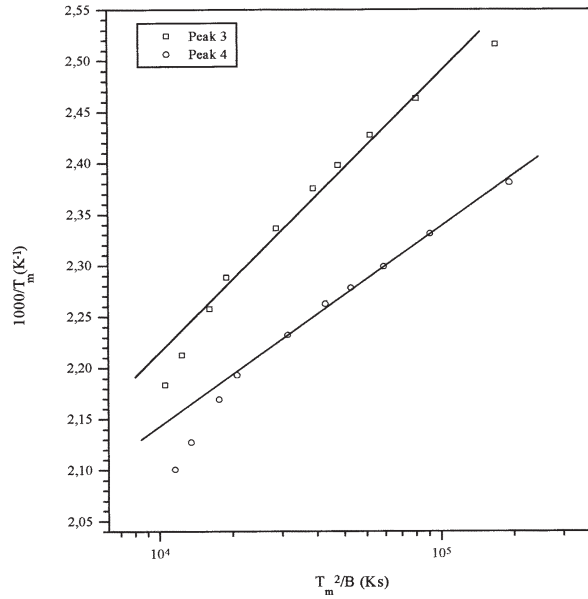


Figure 13. Variable heating rate plots of $1/T_m$ against $\ln(T_m^2/\beta)$ for peak 3 and 4 in TLD-200.

4.3. Dose Level Experiment

It is well known that the trapping parameters highly depend on the shape of the glow peaks, which in turn depend on the applied amount of exposure. Therefore, the radiation quantity is one of the most important experimental parameters in the TL studies. However, up to now, there is no information on the effect of the applied amount of the exposure on the trapping parameters of TL materials in the literature survey. Therefore, in this study, we also investigated the effects of the amount of the dose levels on the trapping parameters of TLD-200. In this respect, Figure 14 shows some of the computer analysed glow curves corresponding to various dose levels such as ≈ 1.2 Gy and ≈ 110 Gy. The individual glow peaks resulting from CGCD procedure are also shown in this figure. The values of E found by CGCD procedure at various dose levels are shown in Figure 15. As in the previous experiments, the variations in the E also start immediately and continue with increasing dose level up to ≈ 40 Gy and then they seem to level off with small up or down changes. Up to ≈ 6 Gy, E of peak 1 considerably drops. Between ≈ 6 Gy and ≈ 25 Gy, its activation energy starts to slowly increase and above ≈ 25 Gy it seems to level off with small up or down changes. On the other hand, E of peak 2 first makes a quick rise up to ≈ 6 Gy, then it seems to level off with increasing dose levels. E of peak 3 reaches to its smooth value (≈ 0.72 eV) at ≈ 10 Gy after some small up or down changes. The variations in E of peak 4 have similar behaviour to the E of peak 3. The variations in E of peak 5 and 6 are very interesting. Up to ≈ 0.3 Gy, E of peak 5 abruptly

decreases, then it always increases with increasing dose level but the increase in E below ≈ 25 Gy is much more significant than above this value. On the other hand, E of peak 6 is continuously decreases with increasing dose level but this decrease at the first part of dose level up to ≈ 25 Gy is much more significant than the later dose level.

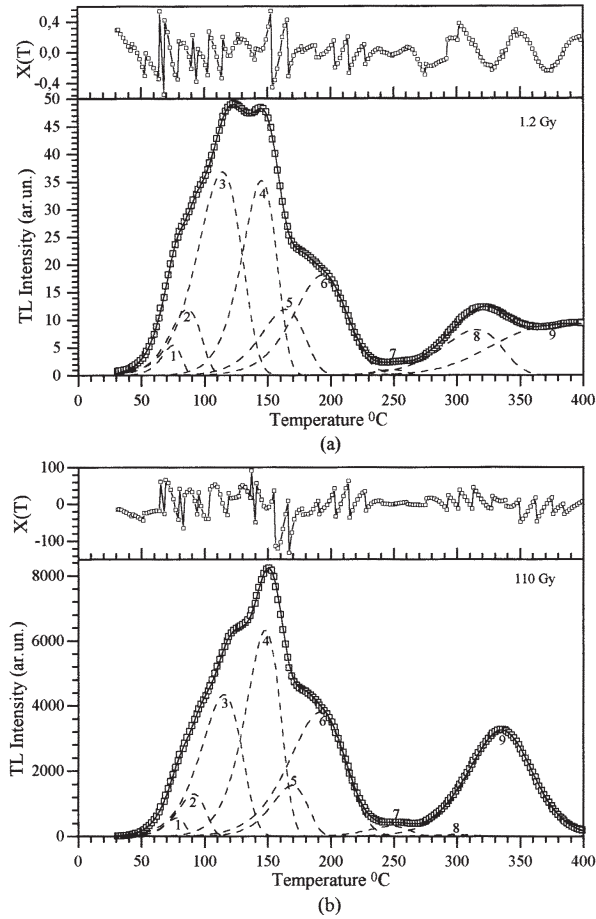


Figure 14. The CGCD analysed glow curves of TLD-200 crystal after various dose levels (a) for 1.2 Gy (FOM=0.42%), (b) for 110 Gy (FOM=0.98%). The open squares represent the experimental points, full curve is the global fitting and broken curves represent fitted individual glow peaks.

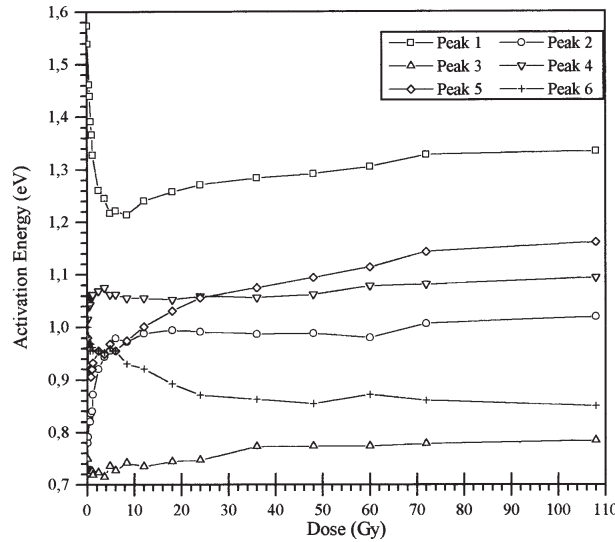


Figure 15. Activation energy E determined by computerised glow curve fitting program versus irradiation duration for glow peaks from glow curves registered at a linear heating rate $1\text{ }^{\circ}\text{C/s}$.

5. Discussion and Conclusion

As seen from Figures 1-15, the analysis of the individual glow peaks of the obtained glow curves reveal the following.

(a) The observations support the assertion that the glow curve is composed of at least 6 glow peaks up to $250\text{ }^{\circ}\text{C}$ below the heating rate $15\text{ }^{\circ}\text{C/s}$.

(b) A significant decrease in the peak area of peak 5 with increasing heating rate. This peak seems to disappear above $15\text{ }^{\circ}\text{C/s}$.

(c) All glow peaks appear to undergo important modifications following storage time at room temperature and with changing heating rate as well as with dose level.

(d) Notable variations in the trapping parameters of all the glow peaks by the experimental parameters.

(e) A considerable change in the kinetic order b of peak 6.

(f) Shifts of the peak maxima of peak 6 to higher temperatures when the annealing time increase at $145 \pm 1\text{ }^{\circ}\text{C}$.

Alterations in the trapping parameters and also peak temperature as a result of annealing and storage times are not expected to occur for alkali halide crystals. The variation in the trapping parameters as a function of annealing time, heating rate and also dose level could have several interpretations:

It was previously mentioned that CGCD method is a very popular method to evaluate the trapping parameters of glow peaks from the glow curves. Because, during the curve fitting procedures whole curve is utilised in the analysis, rather than just a few points

on the glow curve. It is clear that if the number of data points used in the analyses is increased, the greater the potential for accurate determination of the trapping parameters. However, this advantage of CGCD method become offset in some cases, because small distortions in the glow curve yield erroneous trapping parameter values as the computerised fitting routine attempts to define the “best-fit” to the numerical data. The variation in the emission spectrum with temperature, self-absorption, thermal quenching and application of a high heating rate are some possibilities for causing distortions in the glow curve shape which in turn on the trapping parameters of all glow peaks.

Or in the storage times experiments change in trap distributions due to diffusion at room temperature may be the main reason causing variations in the activation energy and consequently their frequency factor and kinetic order. Other factors such as trapped charge conversion from one type of trap to another, completing non-radiation defect interaction may be used for interpreting the drift phenomenon of activation energies. For example, during the application of radiation to the sample, trapped charge conversion from one type of defect to another can take place and these produce many types of defects in the crystal and some of them associate with the previously produced defects and subsequently produce defect complex in the crystal. The presence of these defects distorts the symmetry of the crystal, which in turn distort the band gap of the crystal. These changes then affect the trapping parameters of all glow peaks in TLD-200.

The other factor influencing the glow curves is the heating rate β . The heating rate is a dynamic parameter which affects the characteristics of the TL glow peaks [39]. As the heating rate increases, peak temperature of the glow peaks shifts to higher temperatures, all peaks become broader (FWHM of each peak increases), increasing overlap, and TL intensity measured by the integration method decreases. This decrease in the TL intensity is attributed to the thermal quenching. Any temperature difference across the crystal, not only will give rise to an erroneous shift in the glow peak to higher temperatures, it will also change its shape. When the heating rate increases the temperature lag across the crystal increases very sharply. Therefore, intermediate heating rates ($1^\circ\text{C/s} \leq \beta \leq 20^\circ\text{C/s}$) are chosen in the present study. On the other hand, we have investigated the small temperature differences between the sample and planchet for $\beta > 6^\circ\text{C/s}$ and the exact temperature of the sample has determined using the newly developed method by Kitis and Tuyn [39]. Although the temperature of sample has been corrected using the above method, this result may be explained by the temperature lag influences the shapes of the glow curves at higher readout heating rates ($\beta > 6^\circ\text{C/s}$); which then affects the determination of the trapping parameters by glow curve fitting.

Recently, Kitis *et al.*[19] explained that the kinetic order varies during readout due to the strong variations in the peak temperatures T_{max} and full-width at half maximum (FWHM) with increasing the heating rate. Also, they suggested that these variations affect all other trapping parameters. Therefore, these suggestions can also be used to interpret the drift phenomenon of the kinetic order of peak 6, in the present study.

Another explanation was given by Lewandowski and McKeever [40]. They suggested that temperature dependent kinetic order function with physical significance can be used to substitute the kinetic order. However, in order to understand this variation, it is

necessary to analyse TL glow curve and thermally stimulated conductivity TSC, simultaneously. Additionally, at a low heating rate β_1 , the time spent by the electrons in the CB at any temperature is long enough. As the heating rate increases to $\beta_2 > \beta_1$, the time spent at the same temperatures decreases. So that the retrapping probability of electrons in the CB and also the kinetic order will decrease with increasing heating rates. But it is clear from our calculations that the kinetic order of peak 6 is fractionally between first and second order.

Christodoulides [41] suggested that the general order glow peak may result from traps with the same activation energy and a distribution of the frequency factor. Based on this concept, fluctuation and shift of the distribution of frequency factor during experiment will result in the variation of the estimated frequency factor and subsequent kinetic order. On the other hand, the drift phenomenon of the frequency factor may result from a temperature dependence on the frequency factor and variations of temperature lag due to heating. Therefore, temperature dependence of frequency factor, variations of temperature lag, fluctuation and shift of the distribution frequency factor can be used to interpret the drift phenomenon of the frequency factor. Kinetic order variation during the heating stage can also be used to interpret the drift phenomenon of the frequency factor, because a small change in the kinetic order leads to a change of s by up to one order of magnitude.

Moreover, Piters and Bos [42-43] have suggested that trap defect interaction and defect mobility will result in a distribution of the activation energy and can also influence activation energy. Also, dosimeters from different batches and their impurity concentration and experimental instrumentation such as photo-collecting devices could also influence the shape of glow curves. For example, the photomultiplier tube used in the TL reader does not have the same response at all wavelengths, which then gives rise to a distorted glow curve. It is evident that the different peaks can give rise to emission at different wavelengths.

In order to determine precisely the lifetime of the glow peaks from the obtained values of the trapping parameters, apparently these values must not change with the experimental parameters. It can be concluded that if the trapping parameters for a given TL materials are highly dependent on the experimental parameters the quantitative comparison of calculated and measured fading rates is not straightforward. For example, in the present study, the lifetime of the main peak 4 is determined on the order of 10^2 years. However, it is well known that the actual lifetime of this peak is of order of 10^5 years [4-5]. The same situation is also valid for the other peaks.

As a conclusion, the present experimental study has been shown that many experimental parameters (i.e.; storage times at room temperature, post-irradiation annealing, dose levels and heating rates in the readout stage) have pronounced effects on the determined trapping parameters of all glow peaks in TLD-200 by CGCD method. Therefore all of the above features may go some way to explain why there is such a disagreement between the calculated fading rates (determined from E and s values) and actual fading rates measured in the experimental studies and because of the uncertainties in the trapping parameters it is doubtful whether computerised glow curve analysis of the glow

curves measured with conventional PM tubes can contribute to any extent in a more accurate study of individual glow peaks necessary to gain more information on the radiation quality in mixed radiation fields.

Acknowledgement

The authors are grateful for financial support from the Research Fund of Gaziantep University. We are grateful to Dr.A.J.J.Bos and Dr.T.M.Piters from Interfaculty Reactor Institute, The Netherlands, for providing the CGCD program, and to Dr.G.Kitis for his critical comments on this manuscript.

References

- [1] Mahesh K, Weng P S and Furetta C 1989, *Thermoluminescence in Solids and its Applications*, (Nuclear Technology Publishing Ashford)
- [2] Hsu P C and Wang T K 1986 *Radiation Protection Dosimetry* **16** (3) 253
- [3] Sunta C M 1984 *Radiation Protection Dosimetry* **8** (1/2) 25
- [4] McKeever S W S, Moscovitch M and Townsend P D 1995, *TL Dosimetry Materials: Properties and Uses*, (Nuclear Technology Publishing Ashford)
- [5] McKeever S W S 1985 *Thermoluminescence of Solids* (Cambridge: Cambridge University Press)
- [6] Taylor G C and Lilley E 1978 *J. Phys.D:Appl.Phys.* **11** 567
- [7] Fairchild R G, Mattern P L, Lengweiler K and Levy P W 1978 *J. Appl. Phys.* **49** 4523
- [8] McKeever S W S 1980 *Nucl. Instrum. Methods* **175** 19
- [9] Kathuria S P and Sunta C M 1979 *J. Phys.D:Appl.Phys.* **12** 1573
- [10] Lilley E and McKeever S W S 1983 *J. Phys.D:Appl.Phys* **16** L39
- [11] Dorendrajit Singh S and Gartia R K 1993 *J. Phys.D:Appl.Phys.* **26** 119
- [12] Azorin J and Gutierrez 1986 *Nucl. Tracks* **11** (3) 167
- [13] Souza J H, da Rosa L A R and Mauricio C L P 1993 *Radiation Protection Dosimetry* **47** (1/4) 103
- [14] Bos A J J and Dielhof J B 1993 *Radiation Protection Dosimetry* **37**(4) 231
- [15] Hornyak W F, Levy P W and Kierstead J A 1985 *Nucl. Tracks* **10** (4-6) 557
- [16] Yazici A N, Kayali R and Hacıbrahimoğlu M Y 1998 (*2nd International Kizilirmak Natural Science Congress, Kırkkale TURKEY*) 146
- [17] Bos A J J, Vijverberg R N M, Piters T M and McKeever S W S 1992 *J. Phys.D:Appl. Phys.* **25** 1249

- [18] Shanwen L, Weng P S and Hsu P C 1996 *Appl. Radiat. Isot* **47** (1) 83
- [19] Kitis G, Spiropulu M, Papadopoulos J and Charalambous S 1993 *Nucl. Instruments and Methods in Physic Research* **73** 367
- [20] Yazıcı A N 1998 *Radiation Protection Dosimetry* **80** (4) 379
- [21] Bos A J J, Piters T M, de Vries W and Hoogenboom J E 1990 *Radiation Protection Dosimetry* **33** (1/4) 7
- [22] Bos A J J and Piters T M 1993 *Nucl Tracks Radiat. Meas.* **21** (1) 163
- [23] Ben Shachar B and Horowitz Y S 1995 *J. Phys.D:Appl.Phys.* **28** 1495
- [24] Delgado A G and Gomez Ros J M 1990 *J. Phys.D:Appl.Phys.* **23** 571
- [25] Satinger D, Oster L, Horowitz Y S and Yossian D 1997 *J. Phys.D:Appl.Phys.* **30** 900
- [26] Horowitz Y S and Yossian D 1996 *App. Radiat. Isot.* **47** (8) 825
- [27] Bacci C, Bernardini P, Damilano A, Furetta C and Rispoli 1989 *J. Phys.D:Appl.Phys.* **22** 1751
- [28] Randall J T and Wilkins M H F 1945 *Proc. Roy.Soc.* **A184** 366
- [29] Chen R 1969 *J Appl. Physics* **40** 570
- [30] Grossweiner L I 1953 *J Appl. Physics* **24** 1306
- [31] Halperin A and Braner A A 1960 *Phys. Rev.* **117** 405
- [32] Booth A H 1954 *Can. J. Chem.* **32** 214
- [33] Chen R and Winer A 1970 *J. Appl. Physics* **41** 5227
- [34] Azorin J 1986 *Nucl. Tracks* **11** (3) 159
- [35] Kathuria S P and Sunta C M 1979 *J. Phys.D:Appl.Phys.* **12** 1573
- [36] Bos A J J, Piters J M, Gomez Ros J M and Delgado A 1993 (GLOCANIN, an Intercomparison of Glow Curve Analysis Computer Programs) IRI-CIEMAT Report 131-93-005 IRI Delft
- [37] Misra S K and Eddy N W 1979 *Nucl. Instrum. Methods* **166** 537
- [38] Balian G H and Eddy N W 1977 *Nucl. Instrum. Methods* **145** 389
- [39] Kitis G and Tuyn J W N 1998 *J. Phys.D:Appl.Phys.* **31** 2065
- [40] Lewondowski A C and McKeever S W S 1991 *Phys. Rev.* **B43** 8163
- [41] Christodoulides C 1990 *Phys. Stat. Sol.* **A118** 333
- [42] Piters T M and Bos A J J 1993 *J. Phys.D:Appl.Phys.* **26** 2255
- [43] Piters T M and Bos A J J 1991 *Radiat. Effects Defects in Solids* **119-121** 69